

Fracture Toughness of Polycrystalline Tungsten Alloys

B. Gludovatz^{1,2}, S. Wurster², A. Hoffmann³, R. Pippa^{1,2}

¹*CD Laboratory for Local Analysis of Deformation and Fracture; Leoben, Styria,
Austria*

²*Erich Schmid Institute of Materials Science, Austrian Academy of Sciences;
Leoben, Styria, Austria*

³*Plansee Metall GmbH; Reutte, Tyrol, Austria*

1 Abstract

Tungsten and tungsten alloys show the typical change in fracture behavior from brittle at low temperatures to ductile at high temperatures. In order to improve the understanding of the effect of microstructure the fracture toughness of pure tungsten, potassium doped tungsten, tungsten with 1wt% La₂O₃ and tungsten rhenium alloys were investigated by means of 3-point bending -, double cantilever beam - and compact tension specimens. All these materials show the expected increase in fracture toughness with increasing temperature. The experiments demonstrate that the grain size, texture, chemical composition, grain boundary segregation and dislocation density seem to have a large effect on fracture toughness below the DBTT. These influences can be seen in the fracture behavior and morphology, where two kinds of fracture occur: on one hand the transgranular and on the other hand the intergranular fracture. Therefor techniques like electron backscatter diffraction, auger electron spectroscopy and x-ray line profile analysis were used to improve the understanding of the parameters influencing fracture toughness.

2 Introduction

Most studies related to the ductility of tungsten and tungsten alloys were performed in the sixties and seventies by e.g. Raffo et al. [1]. Since fracture mechanics was not well established at that time the studies on fracture toughness were scarce. Riedle and Gumbsch [2, 3] extensively studied the fracture toughness of tungsten single crystals in the nineties. The effects of crystallographic orientation, crack growing direction, loading rate and temperature were investigated. Compared to the single crystal, the fracture toughness of polycrystalline tungsten is not well examined yet. We started an extensive investigation of the fracture toughness of pure tungsten (W), potassium doped tungsten (AKS-W), tungsten with 1wt% La₂O₃ (WL10) and tungsten-26wt%-rhenium (W26Re). The results of few selected microstructures are presented in this paper. A very large effect of the microstructure especially below the ductile to brittle transition temperature was observed. The investigations indicate that the change from transgranular to intergranular cleavage fracture plays an important role. Especially crystallographic analysis are presented to improve the understanding of interaction of these fracture processes.

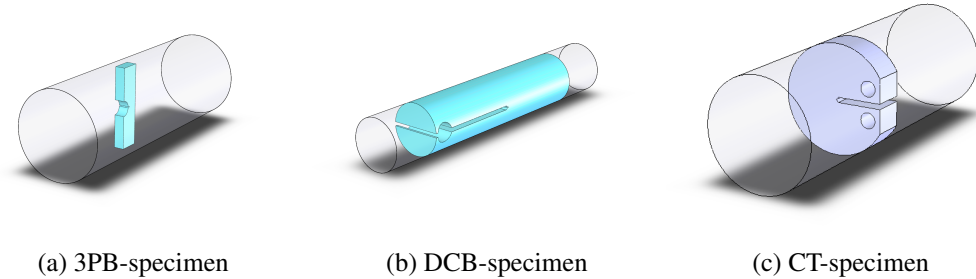


Figure 1: Different specimen types manufactured out of tungsten rods. 3PB-specimen with crack direction in rolling direction (a). DCB-specimen with crack direction in rolling direction (b). CT-specimen with crack direction in tangential direction (c).

3 Experimental

The fracture toughness of W, AKS-W, WL10 and WRe were investigated by means of 3-point bending - (3PB - fig.1-a), double-cantilever beam - (DCB - fig.1-b) and compact tension specimens (CT - fig.1-c). All specimens were manufactured out of rods during different stages of the processing route. Figure 1 shows specimens for tests in rolling- (RD) and tangential direction (TD), additional ones were prepared to investigate the materials in normal direction (ND). The experiments were performed in the range of -196°C to more than 1000°C .

In order to examine the local variation of the fracture resistance DCB-specimen (fig. 2-a) with a length of 30mm, a height of 3.5mm and width of 7.5mm respectively CT-specimen with a length of 7.5mm, a height of 3mm and a width of 6mm were manufactured out of W-, AKS-W-, and WRe-rods. The notches were prepared with a diamond-saw, refined with a razor blade and fatigue-precracked under cyclic compression. The areas in front of the crack-tips were scanned by electron backscatter diffraction (EBSD) after a heat treatment of about 2000°C for an hour in hydrogen atmosphere (fig. 2-b). Some specimens were then loaded under tension within the range of stable crack growth (fig. 2-c). After that the previously scanned areas were scanned again by EBSD (fig. 2-d) to quantify changes of the grain orientation in

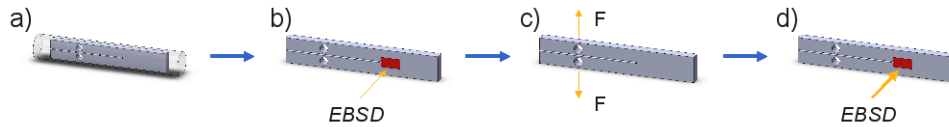


Figure 2: Experimental setup to investigate the local variation of the fracture resistance: Position of a DCB-specimen in a AKS-W rod (a). Scanning the area in front of the crack-tip by EBSD (b). Apply a tensile load on the specimen (c). Scanning the previously scanned area again (d).

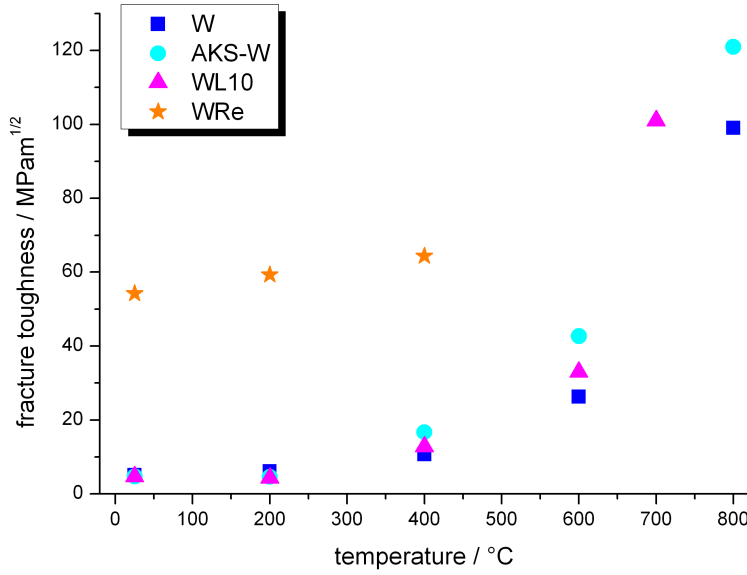


Figure 3: Fracture toughness K_{IC} of W, AKS-W, WL10 (sintered) and W26Re (rolled) as a function of temperature T .

the obtained orientation imaging maps (OIM).

The tests performed at room temperature were done with a microtensile-testing machine of the company *Kammrath & Weiss* while the tests at elevated temperatures were done by use of a *ZWICK* universal-testing machine. The analyses were made by use of a Zeiss 1525 scanning electron microscope equipped with an EDAX EBSD system.

4 Results and Discussion

4.1 Fracture Toughness Investigations

All tested specimens showed the expected increase in fracture toughness with increasing temperature, examples are shown in figure 3. At low temperatures the fracture toughness was determined by use of linear elastic fracture mechanics whereas at temperatures above 600°C the critical crack tip opening displacement $CTOD$ [4] was used to determine the critical stress intensity factor. The fracture toughness determined by stereophotogrammetric techniques is then calculated by

$$K_{IC} = \sqrt{m \cdot \sigma_y \cdot E \cdot COD_C} \quad (1)$$

where σ_y represents the yield strength, E the Young's modulus and m a coefficient which depends on the work hardening factor m of the material. For low hardening m is about 0.5 [5].

Table 1 shows fracture toughness values of CT and 3PB specimens tested at room

Table 1: K_{IC} values of W and W-alloy specimens tested at room temperature

Material	Condition	Rod \varnothing mm	Tests performed	K_{IC} $\text{MPa}\sqrt{\text{m}}$
W	as sintered	23	CT	5.1
	rolled	9	CT (C-R)	4.69
	forged	25	3PB (L-R)	8.01
	rolled	9	3PB (L-R)	9.08
	rolled	4	3PB (L-R)	5.43
	rolled and drawn	1	3PB (L-R)	35.09
WL	as sintered	23	CT	4.72
	rolled	9	CT (C-R)	5.99
	forged	25	3PB (L-R)	16.56
	rolled	9	3PB (L-R)	9.77
	rolled	4	3PB (L-R)	9.74
AKS-W	as sintered	23	CT	6.45
	rolled	9	CT (C-R)	4.50
	rolled	9	3PB (L-R)	32.07
	rolled	4	3PB (L-R)	13.48
	rolled and drawn	1	3PB (L-R)	32.06
WRe (26%)	forged	25	3PB (L-R)	54.24

temperature. The two letter code in the brackets describes the crack plane orientation of different specimens with respect to the geometry of the manufactured material. The first letter designates the *direction normal* to the crack plane, and the second letter the *expected direction of crack propagation* [6]. Due to the extreme differences of the determined K_{IC} values, the processing route seems to have a great influence on the results as well as the direction the specimens have been manufactured out of the rods. Additionally it has to be mentioned that different specimens from the same wires show sometimes large differences. This is probably an effect of the location of the tested volume in the wire of the material as the texture changes from the center to the edge of the wire and also becomes more pronounced the thinner the wires are.

4.2 Examination of the local variation of fracture resistance

For a better understanding of the local variation of the fracture resistance the DCB-specimens were tested with a microtensile-testing - or a universal-testing machine as mentioned earlier. The crack path was recorded by EBSD. In the case of the potassium doped tungsten tested at *RT* the inverse polifigures (IPF) and fracture surfaces show two types of fracture behavior (fig. 4), on one hand the crack propagates intergranular (ig) and on the other hand also transgranular (tg) though the fraction of transgranular crack propagation prevails. Orientation changes within single grains in the interior of an intergranular propagated crack (fig. 4-a) as well as changes within grains in the case of a transgranular propagated crack (fig. 4-b)

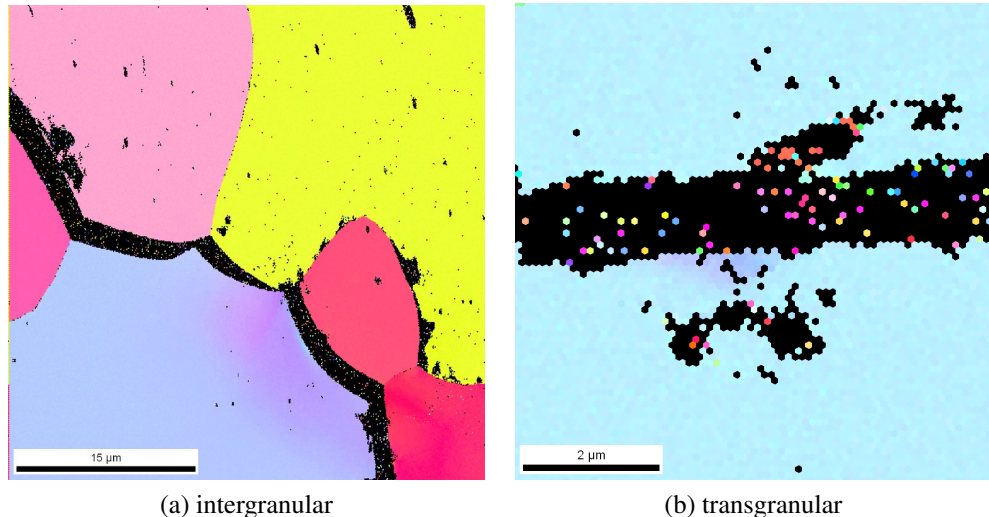


Figure 4: Intergranular (a) and transgranular (b) propagated crack of a DCB-specimen manufactured of AKS-W and tested at RT .

were observed and are clearly viewable through the gradual change in color in both pictures of figure 4. Such deformations are not frequently observable and are just very localized along the crack path of a *RT*-tested specimen.

Figure 5 shows how to correlate the change in orientation with plastic deformation. A narrow band of geometrically necessary dislocations (GND)- generated by the crack tip - is arranged one after the next in a small angle tilt boundary. The volume elements below the boundary are rotated with respect to the elements above. This rotation can be associated with a tilt of crystals which leads to a shear in the direction of the crack propagation [7].

Measurements of the misorientation in the case of the intergranular propagated crack show a maximum value of about 4 degrees whereas the transgranular propagated crack leads to a maximum orientation change of about 5 degrees.

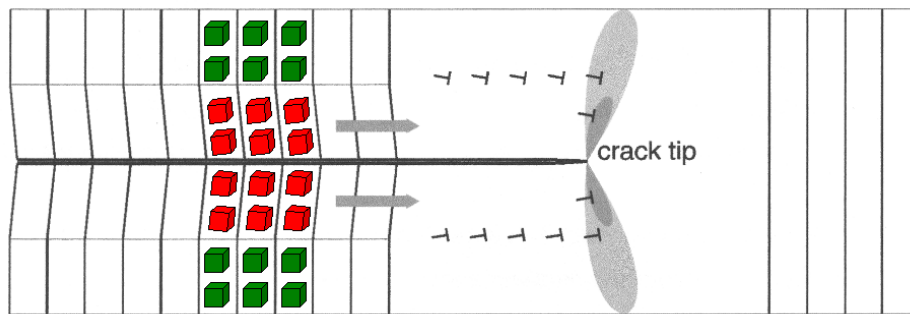


Figure 5: Small angle tilt boundary of geometrically necessary dislocations generated by the crack tip. The tilting of the crystal in the crack-wake can be associated with a shear in the crack propagation direction.

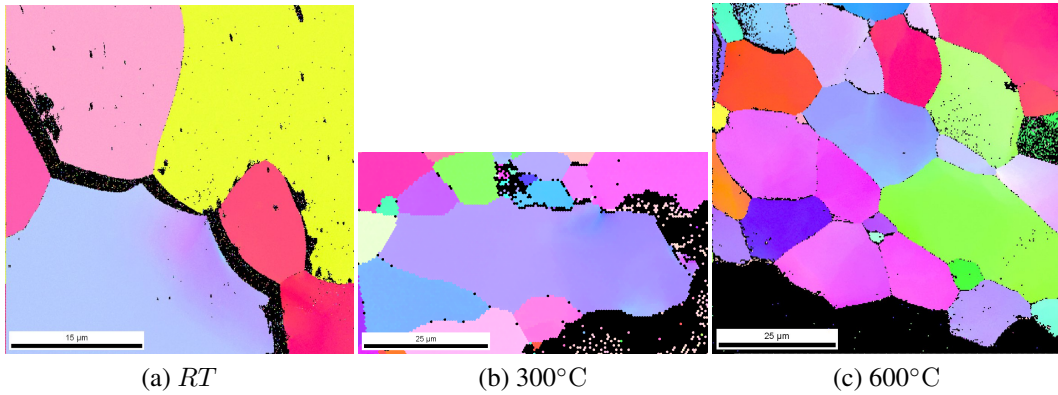


Figure 6: Plastically deformed areas along the crack paths of potassium doped tungsten DCB-specimens tested at *RT* (a), 300°C (b) and 600°C (c).

The DCB-specimens tested at elevated temperatures are shown in figure 6-b/6-c and compared with the specimen tested at *RT* (fig. 6-a). It can be seen that the amount of plastically deformed areas within single grains does not significantly increase from a *RT*-tested specimen to a 300°C-tested specimen or a 600°C-tested specimen. Misorientation measurements within the grains also show that the values are always in the range between 4 and 6 degrees. However the frequency of deformed grains is increasing with increasing temperature. In the case of *RT*- and 300°C-tested specimens the deformation was just observed directly along the crack path whereas the 600°C-tested specimen showed plastically deformed areas also in a wider vicinity of the propagated crack.

The compact tension specimens manufactured of a W26Re alloy were fractured at room temperature and at elevated temperatures. Figure 7 shows scans of all specimens after fracture. Compared to the AKS-W-specimens these IPF show much more plastically deformed areas. Plastically deformed grains in the direct vicinity of the propagated crack were just observed at the *RT*-tested specimen (fig. 7-a). The 300°C- and 600°C-tested samples (fig. 7-b and fig. 7-c) show also plasticification in the wider vicinity of the crack. Measured misorientations of about 10 degrees at

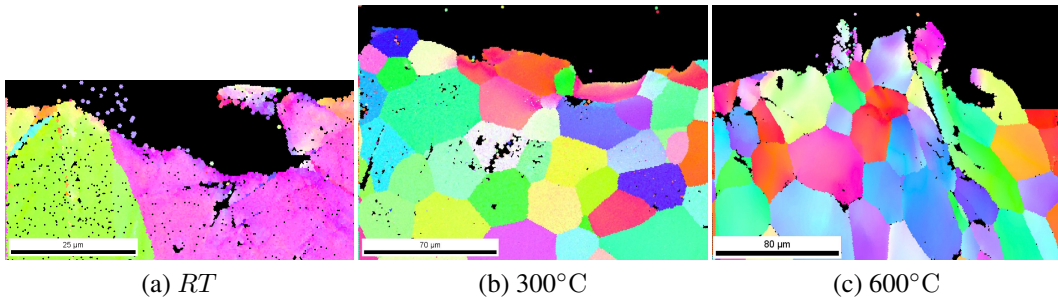


Figure 7: Plastically deformed areas along the crack paths of tungsten rhenium CT-specimens tested at *RT* (a), 300°C (b) and 600°C (c).

the 300°C- and about 14 degrees at the 600°C-tested specimens are much higher than the values of the AKS-W-specimens.

In order to quantify the effect of local varying fracture resistances further investigations on different microstructures will be performed and described in a forthcoming paper.

Acknowledgements

The financial support by the “Christian Doppler Forschungsgesellschaft” is gratefully acknowledged.

A part of this work, supported by the European Communities under the Contract of Association between EURATOM and the Austrian Academy of Sciences, was carried out within the framework of the European Fusion Development Agreement. The views and opinions expressed herein do not necessarily reflect those of the European Commission.

The interesting discussions with Prof. R. Stickler and provided documents is thankfully acknowledged.

References

- [1] P.L. Raffo. Yielding and fracture in tungsten and tungsten-rhenium alloys. *Journal of the Less Common Metals*, 17:133–149, 1969.
- [2] J. Riedle. *Bruchwiderstand in Wolfram-Einkristallen: Einfluss der kristallographischen Orientierung, der Temperatur und der Lastrate*, volume 18: Mechanik/Bruchmechanik. VDI Verlag, 1990.
- [3] P. Gumbsch. Modeling and simulation in materials science. *Summer School of Fracture, Udine (lecture notes)*, 2005.
- [4] O. Kolednik and H.P. Stüwe. The stereophotogrammetric determination of the critical crack tip opening displacement. *Engineering Fracture Mechanics*, 21:145–155, 1985.
- [5] O. Kolednik and H.P. Stüwe. A proposal for estimating the slope of the blunting line. *International Journal of Fracture*, 33:R63–R66, 1987.
- [6] ASTM E 399-90. *Standard Test Method for Plane-Strain Fracture Toughness of Metallic Materials*, Annual Book of ASTM Standards, volume 03.01. American Society for Testing and Materials, 1991.
- [7] R. Pippan, G. Strobl, H. Kreuzer, and C. Motz. Asymmetric crack wake plasticity - a reason for roughness induced crack closure. *Acta Materialia*, 52:4493–4502, 2004.